



# An investigation of Fokas system using two new modifications for the trigonometric and hyperbolic trigonometric function methods

Adnan Ahmad Mahmud<sup>1</sup> · Kalsum Abdulrahman Muhamad<sup>1</sup> · Tanfer Tanriverdi<sup>1</sup> · Hacı Mehmet Baskonus<sup>2</sup>

Received: 30 November 2023 / Accepted: 15 January 2024 / Published online: 11 March 2024  
© The Author(s) 2024

## Abstract

In this work, two new adaptations for the trigonometric and hyperbolic trigonometric function approaches have been presented. These two modifications, entitled modified extended rational sin–cos function technique and modified extended rational sinh–cosh function method, have been applied for the first time to the Fokas system that represents the nonlinear pulse propagation in monomode fiber optics. We intend to produce innovative, explicit traveling waves, solitons, and periodic wave solutions. These achieved outcomes are presented in the form of exponential functions, trigonometric hyperbolic functions, and combination constructions of the exponential functions along with the trigonometric and hyperbolic trigonometric functions. The obtained solutions reveal significant features of the physical phenomenon and are new. The investigated model incorporates the notions of dispersion, transverse diffusion, degree of dispersion, nonlinear pairing, nonlinear immersion, and the force of the nonlinear interaction among the two components of the system. For the most accurate visual evaluation of the physical importance and dynamic properties, we have presented the findings in a variety of plots, which involve two- and three-dimensional representations. One or more elements in our research that are unique, such as newly modified methodologies, is a new observation that leads researchers to invest in new solutions.

**Keywords** Fokas system · Traveling wave transformation · Modified extended rational sinh–cosh function method · Monomode fiber optics · Modified extended rational sin–cos

**Mathematics Subject Classification** 35C07 · 35Dxx · 45Kxx · 65Mxx · 45K05

## 1 Introduction

In the present day of computer networking and communications, the topic of study in the theory of solitons and their utilization in fiber optics is becoming increasingly essential. An optical soliton is a flash of light that travels without distortion owing to dispersion or other causes. Both temporal and spatial solitons will be addressed, combined with the physical

components that make them feasible. In this situation, the optical pulse could begin to create a stable nonlinear pulse known as an optical soliton. The dispersion of the fiber material restricts the bit rate of transmission. Fiber loss is the sole element that contributes to the decline of the pulse quality through expansion in the pulse width.

The complex nonlinear (2 + 1)-dimensional Fokas system that demonstrates nonlinear pulse propagation in monomode fiber optics has the following form:

$$\begin{aligned}iu_t + \beta_1 u_{xxx} + \beta_2 uv &= 0 \\ \beta_3 v_y - \beta_4 (|u|^2)_x &= 0,\end{aligned}\tag{1}$$

that derived in 1994 by Fokas (1994) employing the inverse spectral method, the non-linear pulse propagation in monomode fiber optic is represented by the complex functions  $v(x, y, t)$  and  $u(x, y, t)$ .  $\beta_1$  symbolizes the dispersion coefficient, which characterizes the degree of dispersion in the system,  $\beta_2$  denotes the nonlinear pairing parameter, which indicates the intensity of the nonlinear dealing among the two components of the system,  $u$  and  $v$ ,  $\beta_3$  symbolizes the transverse diffusion parameter, which specifies the amount of dispersion in the transverse direction,  $\beta_4$  illustrates the nonlinear immersion coefficient, which represents the amount of a saturated state of the nonlinear participation. Differing versions of (1) have been examined using various methodologies, including Riccati expansion and Ansatz methods (Khater 2021), the generic Kudryashov's method, the Sardar sub-equation approach, and Bernoulli sub-equation function method (Ali et al. 2023b), the truncated Painlevé approach (Thilakavathy et al. 2023), generalized Riccati equation mapping and Kudryashov methods (Kumar and Kumar 2023a), using a modified mapping method (Mohammed et al. 2023), the extended rational versions of sinh–cosh and sin–cos methods (Wang et al. 2022), the bilinear transformation method (Chen et al. 2019; Rao et al. 2015), the bilinear Kadomtsev–Petviashvili hierarchy reduction method (Rao et al. 2021), the bilinear forms of Hirota's method (Rao et al. 2019), the exponential function method (Wang 2022), the elliptic function expansion forms of the Jacobian method (Tarla et al. 2022), the singular manifold, and the expansion forms of  $G'/G^2$ , Sine-Gordon methods (Alrebdi et al. 2022), the polynomial method that depends on the complete discrimination (Zhang et al. 2023).

Numerous research works examine considerable analytical and semi-analytical techniques for getting the exact solution of NPDEs, including the modified version of the exponential-function method (Muhamad et al. 2023), the extended rational forms of sin–cos and sinh–cosh methods (Mahmud et al. 2023a, b), Bernoulli and its improved version (Baskonus et al. 2022a, b; Mahmud et al. 2023c, d), The transformation of Laplace has been used for solving the fractional system in the form of Caputo fractional derivatives (Tanriverdi et al. 2021), it is worth mentioning that the main source of these modifications are (Mahmud 2023; Muhamad 2023f), the extended auxiliary equation mapping and extended direct algebraic methods (Iqbal et al. 2018a, b, 2019; Seadawy et al. 2019, 2020a, b; Seadawy and Iqbal 2021), the extension of the modified rational expansion method (Seadawy et al. 2021), the modification form of extended auxiliary equation mapping method (Lu et al. 2018; Iqbal and Seadawy 2020; Seadawy and Iqbal 2023), the extended modified rational expansion method (Seadawy et al. 2022), the generalized exponential rational function method (Ghanbari and Gómez-Aguilar 2019a, b; Ghanbari and Baleanu 2020; Ghanbari 2019; Ghanbari et al. 2018; Ghanbari and Kuo 2019; Ghanbari and Baleanu 2019), the five methods mentioned therein (Khater and Ghanbari 2021), the reproducing kernel method (Ghanbari and Akgül 2020), the extended rational sinh-Gordon method and  $\exp(-\phi(\eta))$  expansion function method (Shafqat-ur-Rehman and Ahmad 2023; Rehman and Ahmad

2023), the modified generalized exponential rational function method, and the modified rational sinh–cosh and sin–cos methods (Rehman et al. 2022, 2023a, b; Ahmad et al. 2023; Ahmad 2023), the modified Sardar sub-equation method (Ali et al. 2023a). Considering this context, we can notice an array of methodologies used by several academics to express their ideas in exploring the mathematical models that describe situations in real life (Gasmi et al. 2023; Jafari et al. 2023; Srinivasa and Mundewadi 2023; Bilal et al. 2023; Kumar and Kumar 2023b; Nasir et al. 2023). Overall, some shortcomings and adverse characteristics in the prior versions of these methods became the motivation for us to come up with these two additional enhancements.

This scholarly investigation has been laid out as follows: Sect. 1 is specialized for listing the literature relevant to the approaches and the examined model in a short overview. The methodologies of the described approaches are detailed in Sect. 2. The formulation of the recommended techniques for constructing specific semi-analytic solutions to Eq. (1) is presented in Sect. 3. In Sect. 4, the concluding remarks of the study have been provided agreeably. Finally, the last Sect. 5, is dedicated to the analysis and discussion of the results that were collected.

## 2 Formulation of the modification methods

Always, the configuration of the presented approaches commonly depends on the following step:

*Step 1* Let the next NPDE be followed.

$$\mathcal{A}(\mathcal{I}, \mathcal{I}_x, \mathcal{I}_t, \mathcal{I}_y, \mathcal{I}_{xt}, \mathcal{I}_{xx}, \mathcal{I}_{yt}, \mathcal{I}_{xyt}, \dots) = 0, \tag{2}$$

wherein  $\mathcal{I} = \mathcal{I}(x, y, t)$ . By setting

$$\mathcal{A}(x, y, t) = \mathcal{R}(\mathcal{P}), \quad \mathcal{P} = \delta_1 x + \delta_2 y - \delta_3 t, \tag{3}$$

where  $\delta_1, \delta_2$  and  $\delta_3$  are non-zero arbitrary parameters. If (3) is substituted in (2), then the outcome is presented as follows

$$\mathcal{A}(\mathcal{R}, \mathcal{R}', \mathcal{R}'', \dots) = 0, \tag{4}$$

herein

$$\mathcal{R} = \mathcal{R}(\mathcal{P}), \quad \mathcal{R}' = \frac{d\mathcal{R}}{d\mathcal{P}}, \quad \mathcal{R}'' = \frac{d^2\mathcal{R}}{d\mathcal{P}^2}, \dots$$

*Step 2* Initially, we created these two modified solution forms:

1. For the first modification, let the solution to (4) take the following forms:

$$\mathcal{A}(\mathcal{P}) = \frac{\gamma_0 + \gamma_1 \sinh(\mu \mathcal{P})}{\gamma_2 \sinh(\mu \mathcal{P}) \pm \gamma_3 \cosh(\mu \mathcal{P})}, \quad \gamma_2 \sinh(\mu \mathcal{P}) \pm \gamma_3 \cosh(\mu \mathcal{P}) \neq 0, \tag{5}$$

or,

$$\mathcal{A}(\mathcal{P}) = \frac{\gamma_0 + \gamma_1 \cosh(\mu \mathcal{P})}{\gamma_2 \sinh(\mu \mathcal{P}) \pm \gamma_3 \cosh(\mu \mathcal{P})}, \quad \gamma_2 \sinh(\mu \mathcal{P}) \pm \gamma_3 \cosh(\mu \mathcal{P}) \neq 0, \tag{6}$$

2. For the second modification, suppose that the solutions to (4) take the following forms:

$$\mathcal{R}(\mathcal{P}) = \frac{\gamma_0 + \gamma_1 \sin(\mu \mathcal{P})}{\gamma_2 \sin(\mu \mathcal{P}) \pm \gamma_3 \cos(\mu \mathcal{P})}, \gamma_2 \sin(\mu \mathcal{P}) \pm \gamma_3 \cos(\mu \mathcal{P}) \neq 0, \tag{7}$$

or,

$$\mathcal{R}(\mathcal{P}) = \frac{\gamma_0 + \gamma_1 \cos(\mu \mathcal{P})}{\gamma_2 \sin(\mu \mathcal{P}) \pm \gamma_3 \cos(\mu \mathcal{P})}, \gamma_2 \sin(\mu \mathcal{P}) \pm \gamma_3 \cos(\mu \mathcal{P}) \neq 0, \tag{8}$$

where in (5–8), the  $\mu, \gamma_i$ , for  $i = 0, 1, 2, 3$  are intended coefficients that will be identified later such that

$$\gamma_0^2 + \gamma_1^2 \neq 0, \gamma_2^2 + \gamma_3^2 \neq 0,$$

and a wave number  $\mu \neq 0$ .

*Step 3* Anonymous, also known as parameters, might be found by substituting one of (5–8) into (4), putting together all the terms that have the same powers as and equating to zero all the coefficients for the same power terms, this process produces a set of algebraic equations. Identifying the solutions to the obtained algebraic system using different symbolic computing tools is possible.

*Step 4* By re-installing the obtained results of  $\gamma_0, \gamma_1, \gamma_2, \gamma_3$  and  $\mu$  into one of (5–8), the solution to (4) will be derived, and thereafter, the solution to (2) is obtained.

### 3 Implementations of the recommended methods

Implementing waveform transformation

$$u(x, y, t) = U(\xi)e^{i\kappa\xi}, v(x, y, t) = V(\xi), \xi = \delta_1x + \delta_2y - \delta_3t, \tag{9}$$

to (1), then one gets the following:

$$\begin{aligned} \kappa\delta_3U - i(\delta_3 - 2\beta_1\kappa\delta_1^2)U' - \beta_1\kappa^2\delta_1^2U + \beta_1\delta_1^2U'' + \beta_2UV &= 0 \\ \beta_3\delta_2V' - 2\beta_4\delta_1UU' &= 0. \end{aligned} \tag{10}$$

directly from the second part of (10), one obtains:

$$V = \frac{\beta_4\delta_1}{\beta_3\delta_2}U^2. \tag{11}$$

By substituting (11) into the first part of (10), the following is the outcome:

$$\kappa\delta_3U - i(\delta_3 - 2\beta_1\kappa\delta_1^2)U' - \beta_1\kappa^2\delta_1^2U + \beta_1\delta_1^2U'' + \frac{\beta_2\beta_4\delta_1}{\beta_3\delta_2}U^3 = 0. \tag{12}$$

By splitting the real and imagined components of (12), the operators end up with:

$$\begin{aligned} \kappa\delta_3U - \beta_1\kappa^2\delta_1^2U + \beta_1\delta_1^2U'' + \frac{\beta_2\beta_4\delta_1}{\beta_3\delta_2}U^3 &= 0 \\ -i(\delta_3 - 2\beta_1\kappa\delta_1^2)U' &= 0. \end{aligned} \tag{13}$$

From the imaginary part of (13), one immediately obtains:

$$\kappa = \frac{\delta_3}{2\beta_1\delta_1^2}. \tag{14}$$

By substituting (14) into the real part of (13) after simplifications, the following is the result:

$$\frac{\delta_3^2}{4\beta_1\delta_1^2}U + \beta_1\delta_1^2U'' + \frac{\beta_2\beta_4\delta_1}{\beta_3\delta_2}U^3 = 0. \tag{15}$$

A recommended equation to suppose the trial solution is the ordinary differential equation (15).

### 3.1 Implementation of MER sinh–cosh M to the examined model

To solve (1) by employing the MER sinh-cosh M, suppose that (15) has a solution with the following form:

$$\frac{\gamma_1 \sinh(\mu\xi) + \gamma_0}{\gamma_2 \sinh(\mu\xi) + \gamma_3 \cosh(\mu\xi)}. \tag{16}$$

In (16),  $\mu, \gamma_0, \gamma_1, \gamma_2,$  and  $\gamma_3$  are unknown purposeful parameters that must be demonstrated later by taking into account that

$$\mu \neq 0, \gamma_0^2 + \gamma_1^2 \neq 0, \gamma_2^2 + \gamma_3^2 \neq 0,$$

and  $\mu$  is a wave number. Moreover, the derivatives of (16) with respect to  $\xi$  are taking the following forms:

$$U' = \frac{\gamma_1\gamma_3\mu - \gamma_0\mu(\gamma_3 \sinh(\mu\xi) + \gamma_2 \cosh(\mu\xi))}{(\gamma_2 \sinh(\mu\xi) + \gamma_3 \cosh(\mu\xi))^2}, \tag{17}$$

and

$$U'' = -\frac{2(\gamma_3\mu \sinh(\mu\xi) + \gamma_2\mu \cosh(\mu\xi))(\gamma_1\gamma_3\mu - \gamma_0\mu(\gamma_3 \sinh(\mu\xi) + \gamma_2 \cosh(\mu\xi)))}{(\gamma_2 \sinh(\mu\xi) + \gamma_3 \cosh(\mu\xi))^3} - \frac{\gamma_0\mu(\gamma_2\mu \sinh(\mu\xi) + \gamma_3\mu \cosh(\mu\xi))}{(\gamma_2 \sinh(\mu\xi) + \gamma_3 \cosh(\mu\xi))^2}. \tag{18}$$

Subbing (16)–(18) into (15), one gets the following:

$$\left. \begin{aligned}
 & -4\beta_1^2\beta_3\gamma_0\gamma_2^2\delta_2\delta_1^4\mu^2 \sinh^2(\mu\xi) - 4\beta_1^2\beta_3\gamma_0\gamma_3^2\delta_2\delta_1^4\mu^2 \sinh^2(\mu\xi) - 4\beta_1\beta_2\beta_4\gamma_0^3\delta_1^3 \\
 & + 8\beta_1^2\beta_3\gamma_1\gamma_3^2\delta_2\delta_1^4\mu^2 \sinh(\mu\xi) + 8\beta_1^2\beta_3\gamma_1\gamma_2\gamma_3\delta_2\delta_1^4\mu^2 \cosh(\mu\xi) - \beta_3\gamma_0\gamma_3^2\delta_2\delta_3^2 \\
 & + 4\beta_1^2\beta_3\gamma_0\gamma_3^2\delta_2\delta_1^4\mu^2 - 4\beta_1\beta_2\beta_4\gamma_1^3\delta_1^3 \sinh^3(\mu\xi) - \beta_3\gamma_1\gamma_2^2\delta_2\delta_3^2 \sinh^3(\mu\xi) \\
 & - \beta_3\gamma_1\gamma_3^2\delta_2\delta_3^2 \sinh^3(\mu\xi) - 12\beta_1\beta_2\beta_4\gamma_0\gamma_1^3\delta_1^3 \sinh^2(\mu\xi) - \beta_3\gamma_0\gamma_2^2\delta_2\delta_3^2 \sinh^2(\mu\xi) \\
 & - \beta_3\gamma_0\gamma_3^2\delta_2\delta_3^2 \sinh^2(\mu\xi) - 12\beta_1\beta_2\beta_4\gamma_0^2\gamma_1\delta_1^3 \sinh(\mu\xi) - \beta_3\gamma_1\gamma_3^2\delta_2\delta_3^2 \sinh(\mu\xi) \\
 & - 2\beta_3\gamma_1\gamma_2\gamma_3\delta_2\delta_3^2 \sinh^2(\mu\xi) \cosh(\mu\xi) - 2\beta_3\gamma_0\gamma_2\gamma_3\delta_2\delta_3^2 \sinh(\mu\xi) \cosh(\mu\xi) \\
 & - 8\beta_1^2\beta_3\gamma_0\gamma_2\gamma_3\delta_2\delta_1^4\mu^2 \sinh(\mu\xi) \cosh(\mu\xi) - 8\beta_1^2\beta_3\gamma_0\gamma_2^2\delta_2\delta_1^4\mu^2 = 0.
 \end{aligned} \right\} (19)$$

In (19) collecting all the coefficients with the same powers of  $\cosh^{\tau_1}(\mu\mathcal{P}) \sinh^{\tau_2}(\mu\mathcal{P})$  where  $\tau_1, \tau_2 = 0, 1, 2, 3$  and equating them to zero. From the coefficients of  $\cosh^{\tau_1}(\mu\mathcal{P}) \sinh^{\tau_2}(\mu\mathcal{P})$ , one creates a system as given below:

$$\left. \begin{aligned}
 & -8\beta_1^2\beta_3\gamma_0\gamma_2^2\delta_2\delta_1^4\mu^2 + 4\beta_1^2\beta_3\gamma_0\gamma_3^2\delta_2\delta_1^4\mu^2 - 4\beta_1\beta_2\beta_4\gamma_0^3\delta_1^3 - \beta_3\gamma_0\gamma_3^2\delta_2\delta_3^2 = 0, \\
 & 8\beta_1^2\beta_3\gamma_1\gamma_2\gamma_3\delta_1^4\delta_2\mu^2 = 0, \\
 & 8\beta_1^2\beta_3\gamma_1\gamma_3^2\delta_2\delta_1^4\mu^2 - 12\beta_1\beta_2\beta_4\gamma_0^2\gamma_1\delta_1^3 - \beta_3\gamma_1\gamma_3^2\delta_2\delta_3^2 = 0, \\
 & -8\beta_1^2\beta_3\gamma_0\gamma_2\gamma_3\delta_2\delta_1^4\mu^2 - 2\beta_3\gamma_0\gamma_2\gamma_3\delta_2\delta_3^2 = 0, \\
 & -4\beta_1^2\beta_3\gamma_0\gamma_2^2\delta_2\delta_1^4\mu^2 - 4\beta_1^2\beta_3\gamma_0\gamma_3^2\delta_2\delta_1^4\mu^2 - 12\beta_1\beta_2\beta_4\gamma_0\gamma_1^3\delta_1^3 - \beta_3\gamma_0\gamma_2^2\delta_2\delta_3^2 \\
 & - \beta_3\gamma_0\gamma_3^2\delta_2\delta_3^2 = 0, \\
 & -2\beta_3\gamma_1\gamma_2\gamma_3\delta_2\delta_3^2 = 0, \\
 & -4\beta_1\beta_2\beta_4\gamma_1^3\delta_1^3 - \beta_3\gamma_1\gamma_2^2\delta_2\delta_3^2 - \beta_3\gamma_1\gamma_3^2\delta_2\delta_3^2 = 0.
 \end{aligned} \right\} (20)$$

One creates the following cases by solving (20).

Case 1 The following are the parameters that were obtained from solving (20):

$$\begin{aligned}
 \gamma_2 &= -\frac{\sqrt{2\beta_1\beta_3\gamma_3^2\delta_1\delta_2\mu^2 - \beta_2\beta_4\gamma_0^2}}{\sqrt{2}\sqrt{\beta_1}\sqrt{\beta_3}\sqrt{\delta_1}\sqrt{\delta_2}\mu}; \\
 \gamma_1 &= 0; \delta_3 = -2i\beta_1\delta_1^2\mu.
 \end{aligned} \tag{21}$$

The following set of solutions to (1) has been identified by replacing (21) gathering with (16) into (15).

$$u_1 = \frac{\gamma_0 e^{\delta_2\mu y + \delta_1\mu(x + 2i\beta_1\delta_1\mu t)}}{\gamma_3 \cosh(\delta_2\mu y + \delta_1\mu(x + 2i\beta_1\delta_1\mu t)) - \frac{\sqrt{2\beta_1\beta_3\gamma_3^2\delta_1\delta_2\mu^2 - \beta_2\beta_4\gamma_0^2} \sinh(\delta_2\mu y + \delta_1\mu(x + 2i\beta_1\delta_1\mu t))}{\sqrt{2}\sqrt{\beta_1}\sqrt{\beta_3}\sqrt{\delta_1}\sqrt{\delta_2}\mu}}, \tag{22}$$

and

$$v_1 = \frac{\beta_4\gamma_0^2\delta_1}{\beta_3\delta_2 \left( \gamma_3 \cosh(\mu(2i\beta_1\delta_1^2\mu t + \delta_1x + \delta_2y)) - \frac{\sqrt{2\beta_1\beta_3\gamma_3^2\delta_1\delta_2\mu^2 - \beta_2\beta_4\gamma_0^2} \sinh(\mu(2i\beta_1\delta_1^2\mu t + \delta_1x + \delta_2y))}{\sqrt{2}\sqrt{\beta_1}\sqrt{\beta_3}\sqrt{\delta_1}\sqrt{\delta_2}\mu} \right)^2}. \tag{23}$$

Graphs of (22) and (23) where  $\beta_1 = -\frac{8}{3}; \beta_2 = \frac{1}{2}; \beta_3 = \frac{9}{4}; \beta_4 = \frac{2}{3}; \mu = -\frac{2}{3}; \delta_1 = \frac{2}{5}; \delta_2 = -\frac{1}{2}; y = -\frac{3}{2}; \gamma_0 = \frac{5}{2}; \gamma_3 = \frac{1}{2}$ , and  $-20 \leq x \leq 20, -20 \leq t \leq 20$  are given in the following:

For the values of  $t$  that are mentioned below, one reaches:  
 The values of  $t$  are mentioned in the legend below.

Case 2 The following are the parameters that were obtained from solving (20):

$$\begin{aligned} \gamma_0 &= -\frac{\sqrt{\beta_1}\sqrt{\beta_3}\gamma_3\sqrt{\delta_1}\sqrt{\delta_2}\mu}{\sqrt{2}\sqrt{\beta_2}\sqrt{\beta_4}}; \\ \gamma_1 &= -\frac{i\sqrt{\beta_1}\sqrt{\beta_3}\gamma_3\sqrt{\delta_1}\sqrt{\delta_2}\mu}{\sqrt{2}\sqrt{\beta_2}\sqrt{\beta_4}}; \gamma_2 = 0; \delta_3 = -\sqrt{2}\beta_1\delta_1^2\mu. \end{aligned} \tag{24}$$

The following set of solutions to (1) has been determined by re-installing (24) with (16) into (15).

$$\begin{aligned} u_2 = & -\frac{\sqrt{\beta_1}\sqrt{\beta_3}\sqrt{\delta_1}\sqrt{\delta_2}\mu \exp\left(-\frac{i\mu(\sqrt{2}\beta_1\delta_1^2\mu + \delta_1x + \delta_2y)}{\sqrt{2}}\right) \operatorname{sech}\left(\mu\left(\sqrt{2}\beta_1\delta_1^2\mu + \delta_1x + \delta_2y\right)\right)}{\sqrt{2}\sqrt{\beta_2}\sqrt{\beta_4}} \\ & - \frac{\sqrt{\beta_1}\sqrt{\beta_3}\sqrt{\delta_1}\sqrt{\delta_2}\mu \exp\left(-\frac{i\mu(\sqrt{2}\beta_1\delta_1^2\mu + \delta_1x + \delta_2y)}{\sqrt{2}}\right) \left(i \tanh\left(\mu\left(\sqrt{2}\beta_1\delta_1^2\mu + \delta_1x + \delta_2y\right)\right)\right)}{\sqrt{2}\sqrt{\beta_2}\sqrt{\beta_4}}, \end{aligned} \tag{25}$$

and

$$v_2 = \frac{\beta_1\delta_1^2\mu^2\left(\operatorname{sech}\left(\mu\left(\sqrt{2}\beta_1\delta_1^2\mu + \delta_1x + \delta_2y\right)\right) + i \tanh\left(\mu\left(\sqrt{2}\beta_1\delta_1^2\mu + \delta_1x + \delta_2y\right)\right)\right)^2}{2\beta_2}. \tag{26}$$

Profile of the solutions in (25) and (26) where  $\beta_1 = \frac{8}{3}; \beta_2 = \frac{1}{2}; \beta_3 = \frac{5}{4}; \beta_4 = \frac{2}{5}; \mu = -\frac{3}{4}; \delta_1 = \frac{5}{2}; \delta_2 = \frac{3}{2}; y = -\frac{3}{2}; \gamma_0 = \frac{5}{2}; \gamma_3 = \frac{1}{2}$ ; and  $-20 \leq x \leq 20$ , are given below for the different values of  $t$  that mentioned in the legend

Case 3 The following are the parameters that were reached from solving (20):

$$\gamma_0 = -\frac{i\sqrt{\beta_3}\gamma_3\sqrt{\delta_2}\delta_3}{\sqrt{2}\sqrt{\beta_1}\sqrt{\beta_2}\sqrt{\beta_4}\delta_1^{3/2}}; \gamma_1 = 0; \gamma_2 = 0; \mu = \frac{i\delta_3}{2\beta_1\delta_1^2}. \tag{27}$$

By inserting (27) and (16) into (15), the following set of solutions to (1) have been gained:

$$u_3 = -\frac{i\sqrt{\beta_3}\sqrt{\delta_2}\delta_3 \exp\left(\frac{i\delta_3(-\delta_3t + \delta_1x + \delta_2y)}{2\beta_1\delta_1^2}\right) \operatorname{sec}\left(\frac{\delta_3(-\delta_3t + \delta_1x + \delta_2y)}{2\beta_1\delta_1^2}\right)}{\sqrt{2}\sqrt{\beta_1}\sqrt{\beta_2}\sqrt{\beta_4}\delta_1^{3/2}}, \tag{28}$$

and

$$v_3 = -\frac{\delta_3^2 \sec^2\left(\frac{\delta_3(-\delta_3 t + \delta_1 x + \delta_2 y)}{2\beta_1 \delta_1^2}\right)}{2\beta_1 \beta_2 \delta_1^2}. \tag{29}$$

**Remark 1** Similarly, by assuming that (6) is the trial solution to (15), some other set solutions to (1) may be obtained using the same prior process.

### 3.2 Implementation of MER sin–cos M to the examined model

To solve (1) by employing the MER sin–cos M, suppose that (15) has a solution with the following structure:

$$\frac{\lambda_1 \cos(\mu \xi) + \lambda_0}{\lambda_3 \sin(\mu \xi) + \lambda_2 \cos(\mu \xi)}. \tag{30}$$

In (16),  $\mu$ ,  $\lambda_0$ ,  $\lambda_1$ ,  $\lambda_2$ , and  $\lambda_3$  are unknown purposeful parameters that must be demonstrated later by taking into account that

$$\mu \neq 0, \lambda_0^2 + \lambda_1^2 \neq 0, \lambda_2^2 + \lambda_3^2 \neq 0,$$

and  $\mu$  is a wave number. Moreover, the successive derivatives of (16) according to  $\xi$  are taking the forms below.

$$U' = \frac{\lambda_0 \lambda_2 \mu \sin(\mu \xi) - \lambda_3 \mu (\lambda_0 \cos(\mu \xi) + \lambda_1)}{(\lambda_3 \sin(\mu \xi) + \lambda_2 \cos(\mu \xi))^2}, \tag{31}$$

and

$$U'' = -\frac{2(\lambda_3 \mu \cos(\mu \xi) - \lambda_2 \mu \sin(\mu \xi))(\lambda_0 \lambda_2 \mu \sin(\mu \xi) - \lambda_3 \mu (\lambda_0 \cos(\mu \xi) + \lambda_1))}{(\lambda_3 \sin(\mu \xi) + \lambda_2 \cos(\mu \xi))^3} + \frac{\lambda_0 \lambda_3 \mu^2 \sin(\mu \xi) + \lambda_0 \lambda_2 \mu^2 \cos(\mu \xi)}{(\lambda_3 \sin(\mu \xi) + \lambda_2 \cos(\mu \xi))^2}. \tag{32}$$

Subbing (30)–(32) into (15), one gets the following:

$$\left. \begin{aligned} &4\beta_1^2 \beta_3 \delta_2 \delta_1^4 \lambda_0 \lambda_2^2 \mu^2 \sin^2(\mu \xi) - 4\beta_1^2 \beta_3 \delta_2 \delta_1^4 \lambda_0 \lambda_3^2 \mu^2 \sin^2(\mu \xi) + 4\beta_1 \beta_2 \beta_4 \delta_1^3 \lambda_0^3 \\ &- 8\beta_1^2 \beta_3 \delta_2 \delta_1^4 \lambda_1 \lambda_2 \lambda_3 \mu^2 \sin(\mu \xi) + 8\beta_1^2 \beta_3 \delta_2 \delta_1^4 \lambda_1 \lambda_3^2 \mu^2 \cos(\mu \xi) \\ &- 8\beta_1^2 \beta_3 \delta_2 \delta_1^4 \lambda_0 \lambda_2 \lambda_3 \mu^2 \sin(\mu \xi) \cos(\mu \xi) + 4\beta_1^2 \beta_3 \delta_2 \delta_1^4 \lambda_0 \lambda_2^2 \mu^2 \\ &+ 8\beta_1^2 \beta_3 \delta_2 \delta_1^4 \lambda_0 \lambda_3^2 \mu^2 + \beta_3 \delta_2 \delta_3^2 \lambda_0 \lambda_3^2 \sin^2(\mu \xi) + 4\beta_1 \beta_2 \beta_4 \delta_1^3 \lambda_1^3 \cos^3(\mu \xi) \\ &+ \beta_3 \delta_2 \delta_3^2 \lambda_1 \lambda_2^2 \cos^3(\mu \xi) + 12\beta_1 \beta_2 \beta_4 \delta_1^3 \lambda_0 \lambda_1^2 \cos^2(\mu \xi) + \beta_3 \delta_2 \delta_3^2 \lambda_0 \lambda_2^2 \cos^2(\mu \xi) \\ &+ 12\beta_1 \beta_2 \beta_4 \delta_1^3 \lambda_0^3 \lambda_1 \cos(\mu \xi) + 2\beta_3 \delta_2 \delta_3^2 \lambda_1 \lambda_2 \lambda_3 \sin(\mu \xi) \cos^2(\mu \xi) \\ &+ \beta_3 \delta_2 \delta_3^2 \lambda_1 \lambda_3^2 \sin^2(\mu \xi) \cos(\mu \xi) + 2\beta_3 \delta_2 \delta_3^2 \lambda_0 \lambda_2 \lambda_3 \sin(\mu \xi) \cos(\mu \xi) = 0. \end{aligned} \right\} \tag{33}$$



In (33), by collecting all the coefficients with the same powers of  $\cos^{\tau_1}(\mu \mathcal{P}) \sin^{\tau_2}(\mu \mathcal{P})$  where  $\tau_1, \tau_2 = 0, 1, 2, 3$  and equating them to zero. From the coefficients of  $\cos^{\tau_1}(\mu \mathcal{P}) \sin^{\tau_2}(\mu \mathcal{P})$ , one creates a system as given below:

$$\left. \begin{aligned} 4\beta_1^2\beta_3\delta_2\delta_1^4\lambda_0\lambda_2^2\mu^2 + 8\beta_1^2\beta_3\delta_2\delta_1^4\lambda_0\lambda_3^2\mu^2 + 4\beta_1\beta_2\beta_4\delta_1^3\lambda_0^3 &= 0, \\ -8\beta_1^2\beta_3\delta_1^4\delta_2\lambda_1\lambda_2\lambda_3\mu^2 &= 0, \\ 4\beta_1^2\beta_3\delta_2\delta_1^4\lambda_0\lambda_2^2\mu^2 - 4\beta_1^2\beta_3\delta_2\delta_1^4\lambda_0\lambda_3^2\mu^2 + \beta_3\delta_2\delta_3^2\lambda_0\lambda_3^2 &= 0, \\ 8\beta_1^2\beta_3\delta_2\delta_1^4\lambda_1\lambda_3^2\mu^2 + 12\beta_1\beta_2\beta_4\delta_1^3\lambda_0^2\lambda_1 &= 0, \\ 2\beta_3\delta_2\delta_3^2\lambda_0\lambda_2\lambda_3 - 8\beta_1^2\beta_3\delta_1^4\delta_2\lambda_0\lambda_2\lambda_3\mu^2 &= 0, \\ \beta_3\delta_2\delta_3^2\lambda_1\lambda_3^2 &= 0, \\ 12\beta_1\beta_2\beta_4\delta_1^3\lambda_0\lambda_1^2 + \beta_3\delta_2\delta_3^2\lambda_0\lambda_2^2 &= 0, \\ 2\beta_3\delta_2\delta_3^2\lambda_1\lambda_2\lambda_3 &= 0, \\ 4\beta_1\beta_2\beta_4\delta_1^3\lambda_1^3 + \beta_3\delta_2\delta_3^2\lambda_2^2\lambda_1 &= 0. \end{aligned} \right\} \tag{34}$$

By solving (34), the following cases are created:

*Case 1* The following are the parameters that were obtained from solving (34):

$$\beta_1 = \frac{\delta_3}{2\delta_1^2\mu}; \lambda_1 = 0; \lambda_2 = 0; \lambda_0 = \frac{i\sqrt{\beta_3}\sqrt{\delta_2}\sqrt{\delta_3}\lambda_3\sqrt{\mu}}{\sqrt{\beta_2}\sqrt{\beta_4}\sqrt{\delta_1}}. \tag{35}$$

The following set of solutions to (1) has been identified by replacing (35) gathering with (30) into (15).

$$u_4 = \frac{i\sqrt{\beta_3}\sqrt{\delta_2}\sqrt{\delta_3}\sqrt{\mu}(\cot(\mu(-\delta_3t + \delta_1x + \delta_2y)) + i)}{\sqrt{\beta_2}\sqrt{\beta_4}\sqrt{\delta_1}}, \tag{36}$$

and

$$v_4 = -\frac{\delta_3\mu}{\beta_2} \csc^2(\mu(-\delta_3t + \delta_1x + \delta_2y)). \tag{37}$$

Graphs of (36) and (37) where  $\beta_2 = \frac{1}{4}; \beta_3 = \frac{7}{2}; \beta_4 = \frac{5}{3}; \mu = \frac{1}{2}; \delta_1 = \frac{2}{5}; \delta_2 = \frac{3}{2}; \delta_3 = \frac{3}{4}; y = \frac{3}{2}$ , and  $-10 \leq x \leq 10, -10 \leq t \leq 10$  are given in the following:

Where the values of  $t$  are mentioned in the legend, one gets:

*Case 2* The following are the parameters that were obtained from solving (34):

$$\delta_1 = \frac{i\sqrt{\delta_3}}{\sqrt{2}\sqrt{\beta_1}\sqrt{\mu}}; \lambda_1 = 0; \lambda_2 = 0; \lambda_0 = \frac{i\sqrt{-2}\sqrt{\beta_1}\sqrt{\beta_3}\sqrt{\delta_2}\sqrt{\delta_3}\lambda_3\mu^{3/4}}{\sqrt{\beta_2}\sqrt{\beta_4}}. \tag{38}$$

The following set of solutions to (1) has been determined by re-installing (38) with (30) into (15).

$$u_5 = \frac{2^4 \sqrt{-2} \sqrt{\beta_1} \sqrt{\beta_3} \sqrt{\delta_2} \sqrt{\delta_3} \mu^{3/4} e^{\frac{\sqrt{2} \sqrt{\beta_3} \sqrt{\mu x}}{\sqrt{\beta_1}} + 2i \delta_3 \mu t}}{\sqrt{\beta_2} \sqrt{\beta_4} \left( e^{\frac{\sqrt{2} \sqrt{\beta_3} \sqrt{\mu x}}{\sqrt{\beta_1}} + 2i \delta_3 \mu t} - e^{2i \delta_2 \mu y} \right)}, \tag{39}$$

and

$$v_5 = \frac{\delta_3 \mu}{\beta_2} \operatorname{csc}^2 \left( \mu \left( -\delta_3 t + \frac{i \sqrt{\delta_3} x}{\sqrt{2} \sqrt{\beta_1} \sqrt{\mu}} + \delta_2 y \right) \right). \tag{40}$$

Profile of the solutions in (39) and (40) where  $\beta_1 = \frac{8}{3}; \beta_2 = \frac{1}{8}; \beta_3 = -\frac{1}{4}; \beta_4 = \frac{2}{5}; \mu = \frac{1}{2}; \delta_1 = \frac{5}{2}; \delta_2 = -\frac{1}{2}; \delta_3 = \frac{5}{2}; y = -\frac{3}{2}$  and  $-20 \leq x \leq 20, -20 \leq t \leq 20$  are given below:

For the values of  $t$  that are mentioned in the legend, one reaches:

For the values of  $t$  that are mentioned in the legend, one obtains:

**Remark 2** Similarly, by assuming that (7) is the trial solution to (15), some other set solutions to (1) may be obtained using the same prior process.

### 4 Conclusion

The present study describes the first implementation of two modified trigonometric analytic methods on a complex nonlinear (2 + 1)-dimensional Fokas system. The studied model is constructed to explain the nonlinear pulsed transmission in monomode fibers with optical features. Our novel modification approaches are the modified extended rational sinh–cosh method and the modified extended rational sin–cos method. The outcomes have been illustrated by numerous innovative and unique solutions that have been stated by traveling waves, oscillating, soliton types, and exponential rational functions blended with trigonometric and hyperbolic trigonometric functions. The updated approaches are trustworthy, influential, and straightforward in discovering semi-analytic solutions to mathematical models in numerous domains, such as mathematics, physics, biology, and engineering. The detected results have been detailed in three dimensions, contour surfaces, and two-dimensional graphs that represent the impact of temporal progression. The two- and three-dimensional displays help us better appreciate the qualities of the acquired outcomes. The obtained outcomes have all been properly validated by putting the created findings back into their linked equations. The functioning and behavior of the graphs mostly rely on the specified numerical values that are supplied for the optional coefficients. For the future scope of the work, we recommend that the authors use these two modifications, which we believe are useful, practical, and effective. It will play a significant role in forthcoming research related to applied science.

### 5 Results and discussion

The following statements have been added to clarify the distinguishing characteristics of our updating methods: We have acquired a collection of solutions that are difficult to get through the utilization of prior iterations of these techniques. The adjustments we have

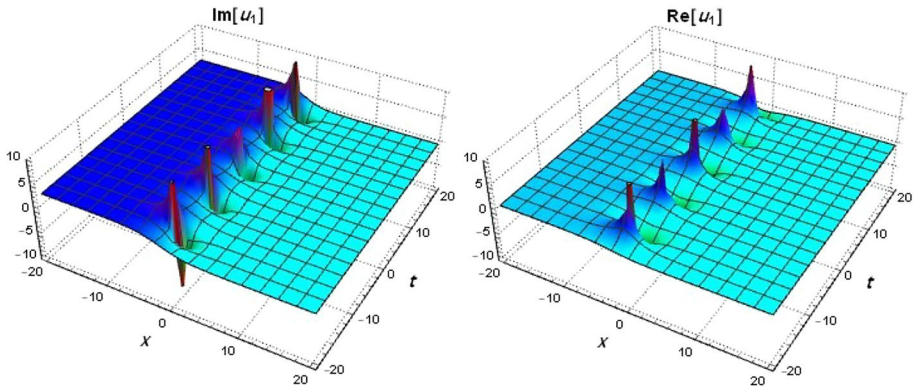


Fig. 1 3D figures of (22)

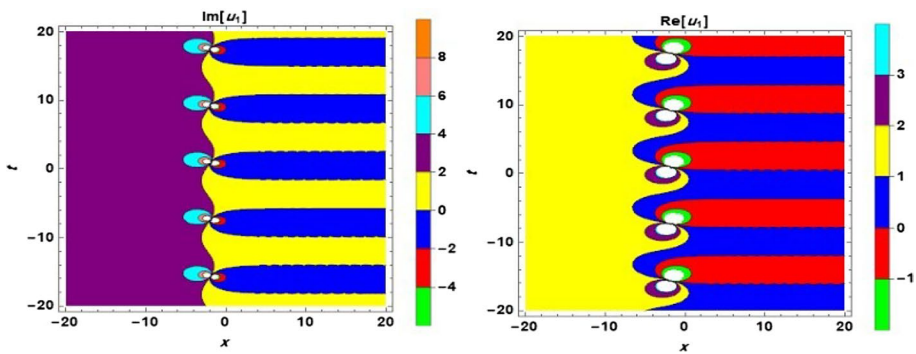


Fig. 2 Contour surfaces of (22)

made are dependable, efficient, and swiftly adaptable to many mathematical models. Some shortcomings and unfavorable variables in the past versions of these procedures supplied the impetus for us to arrive at these two further enhancements. Although no analytical technique is devoid of drawbacks, positively, there are major benefits to our modifications for portraying the formulated solution in (22) and in (23) that are unreachable to acquire by employing the prior old versions. The singular breather solitons in both  $x$  and  $t$  are shown in Figs. 1, 2, 3, 4 and 5. Figure 6 represents a solitary wave on the left and a bright soliton on the right-hand side. Figures 7, 8, 9, 10 and 11 represent periodic and traveling wave solutions. The two interacting breather solitons are illustrated in Figs. 12, 13 and 14. The dark soliton on the right-hand side and the solitary waveform on the left-hand side can be observed in Figs. 15, 16 and 17.

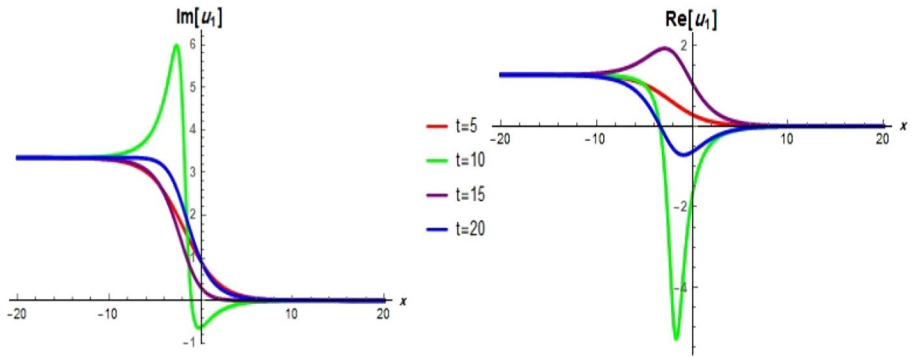


Fig. 3 2D graphs of (22)

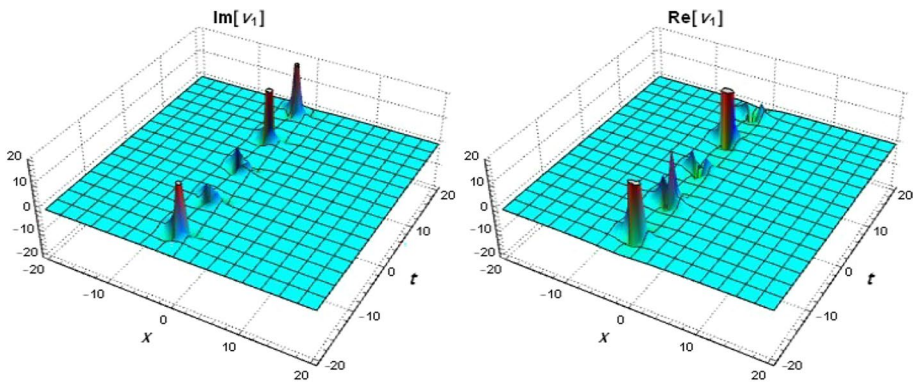


Fig. 4 3D figures of (23)

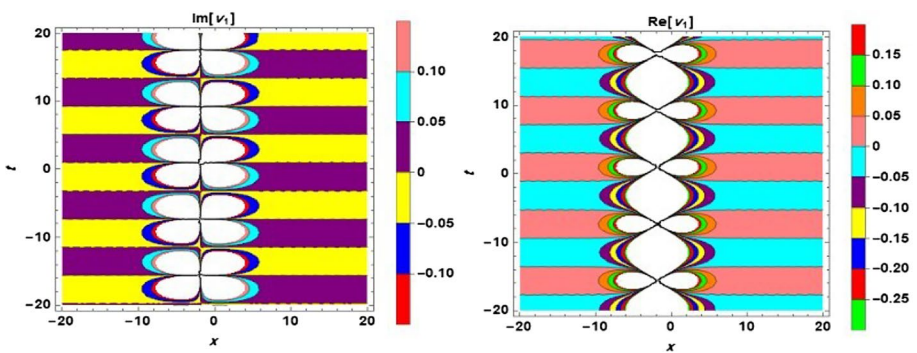


Fig. 5 Contour surfaces of (23)

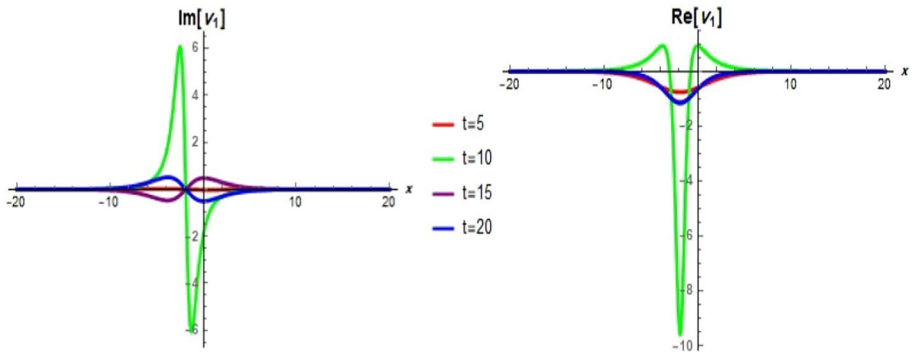


Fig. 6 2D graphs of (23)

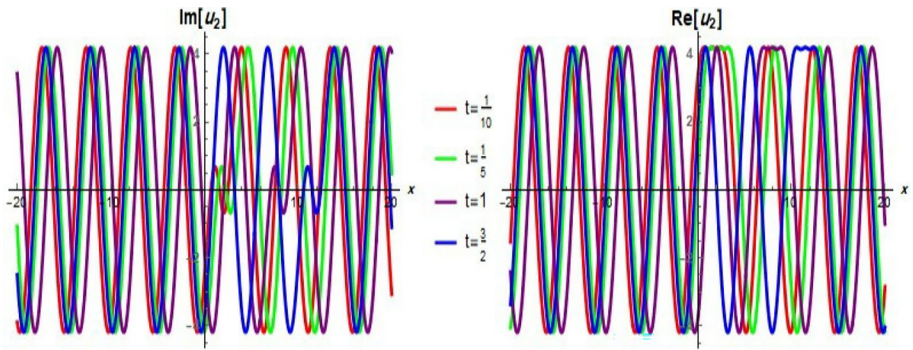


Fig. 7 2D graphs to (25)

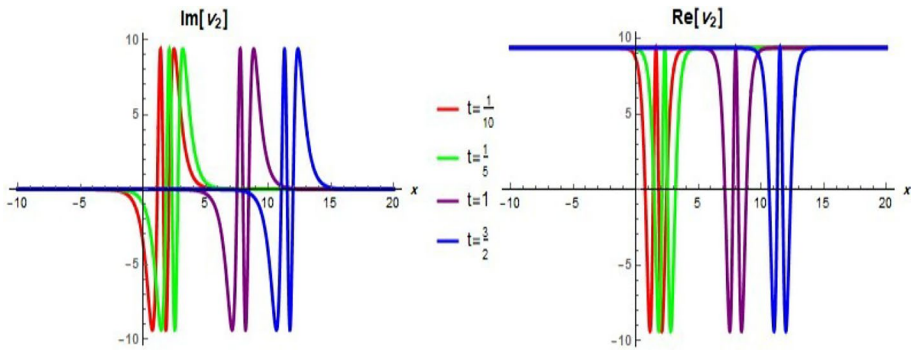


Fig. 8 2D graphs to (26)

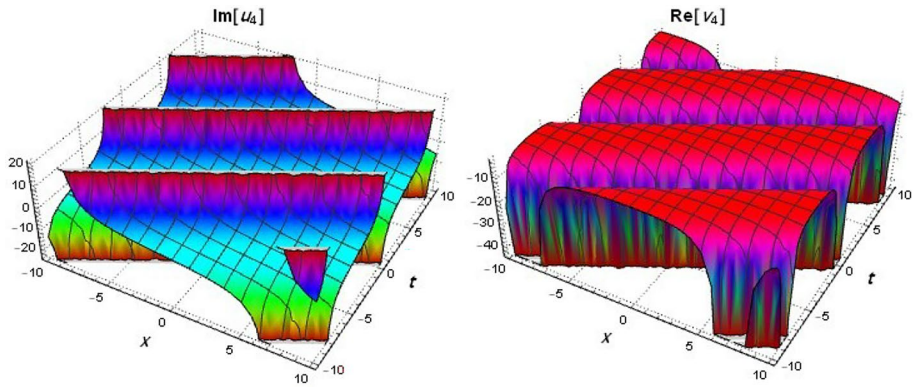


Fig. 9 3D figures represent the imaginary part of (36) and the real part of (37)

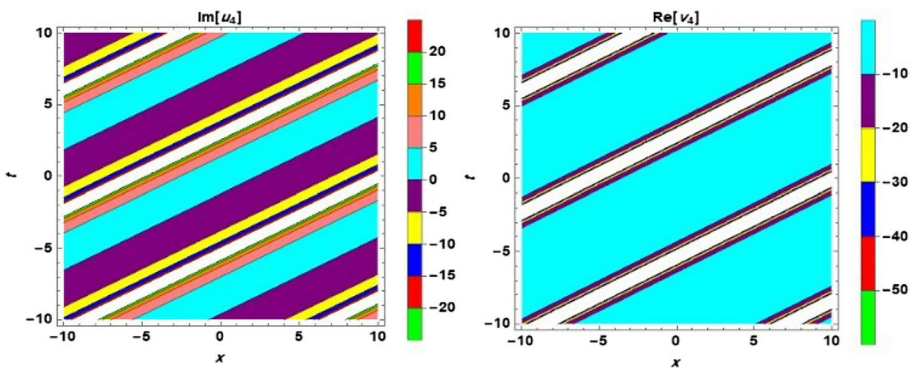


Fig. 10 Contour surfaces represent the imaginary part of (36) and the real part of (37)

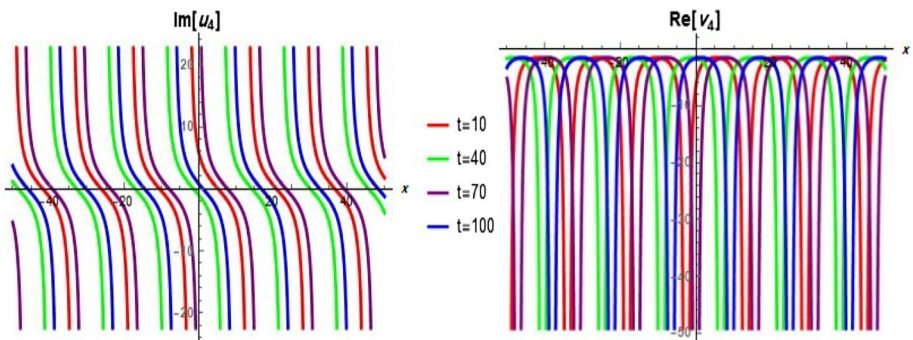


Fig. 11 2D graphs represent the imaginary part of (36) and the real part of (37)

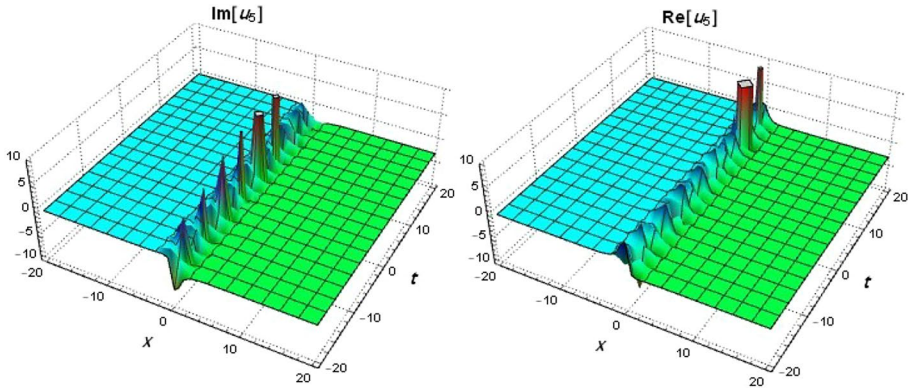


Fig. 12 3D figures of (39)

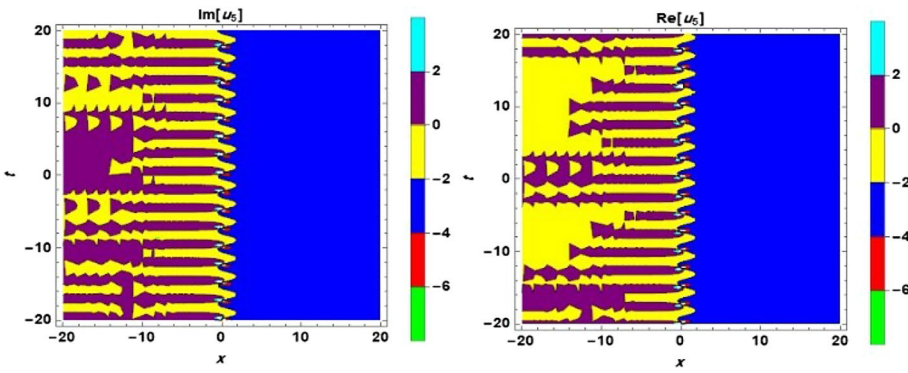


Fig. 13 Contour surfaces of (39)

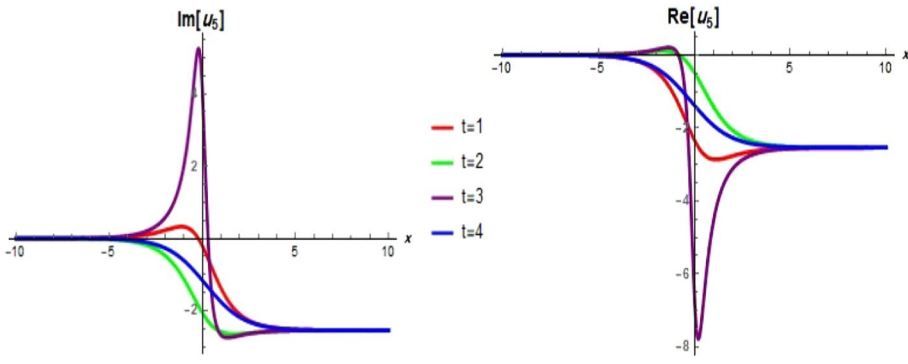


Fig. 14 2D graphs of (39)

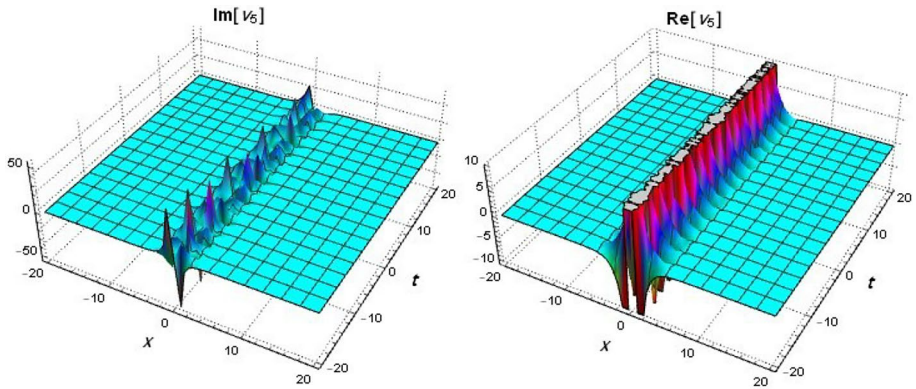


Fig. 15 3D figures of (40)

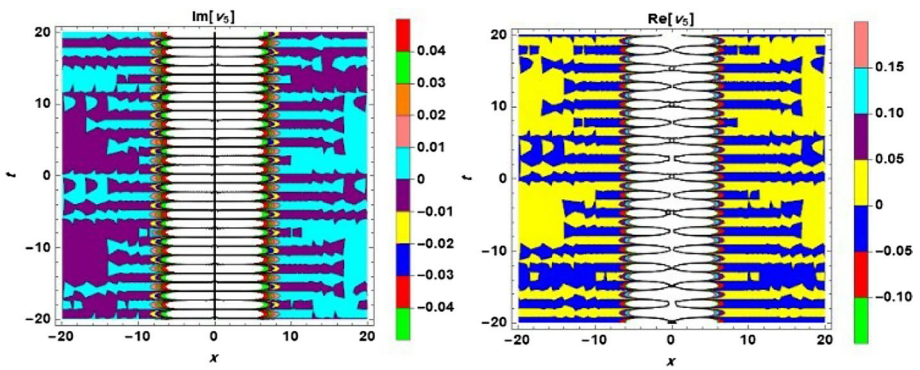


Fig. 16 Contour surfaces of (40)

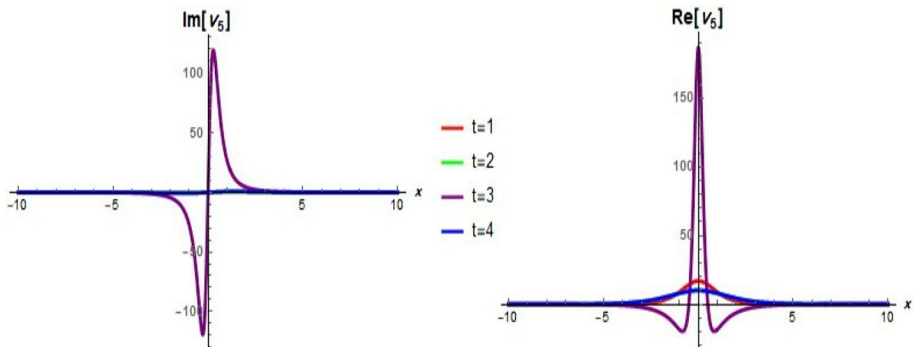


Fig. 17 2D graphs of (40)



**Acknowledgements** All the authors are appreciative of the respective editor and all reviewers for their valuable comments and the conducive research environment that greatly facilitated the completion of this work.

**Author contributions** The authors investigated the research model, developed applications, and performed calculations. All authors contributed equally to the writing of the paper and equally to the assessment of the results.

**Funding** Open access funding provided by the Scientific and Technological Research Council of Türkiye (TÜBİTAK). No funding is available for this work presented in this manuscript.

**Data availability** There are no related data with this paper, or the data will not be deposited. For ethical and legal reasons, the data produced and/or evaluated during the present investigations are not publicly accessible, but they are available from the relevant author upon justifiable request.

## Declarations

**Ethical approval** The authors confirm their adherence to ethical standards.

**Conflict of interest** The authors indicate that there is no conflict between their interests in publishing this work.

**Open Access** This article is licensed under a Creative Commons Attribution 4.0 International License, which permits use, sharing, adaptation, distribution and reproduction in any medium or format, as long as you give appropriate credit to the original author(s) and the source, provide a link to the Creative Commons licence, and indicate if changes were made. The images or other third party material in this article are included in the article's Creative Commons licence, unless indicated otherwise in a credit line to the material. If material is not included in the article's Creative Commons licence and your intended use is not permitted by statutory regulation or exceeds the permitted use, you will need to obtain permission directly from the copyright holder. To view a copy of this licence, visit <http://creativecommons.org/licenses/by/4.0/>.

## References

- Ahmad, J.: Dynamics of optical and other soliton solutions in fiber Bragg gratings with Kerr law and stability analysis. *Arab. J. Sci. Eng.* **48**(1), 803–819 (2023)
- Ahmad, J., Mustafa, Z., Turki, N.B., Shah, N.A., et al.: Solitary wave structures for the stochastic Nizhnik–Novikov–Veselov system via modified generalized rational exponential function method. *Results Phys.* **52**, 106776–106786 (2023)
- Ali, A., Ahmad, J., Javed, S., Rehman, S.-U.: Analysis of chaotic structures, bifurcation and soliton solutions to fractional Boussinesq model. *Phys. Scr.* **98**, 075217–075236 (2023a)
- Ali, K.K., AlQahtani, S.A., Mehanna, M., Bekir, A.: New optical soliton solutions for the  $(2+1)$  Fokas system via three techniques. *Opt. Quantum Electron.* **55**(7), 638–656 (2023b)
- Alrebbi, T.A., Raza, N., Arshed, S., Abdel-Aty, A.-H.: New solitary wave patterns of Fokas-system arising in monomode fiber communication systems. *Opt. Quantum Electron.* **54**(11), 712–731 (2022)
- Baskonus, H.M., Mahmud, A.A., Muhamad, K.A., Tanriverdi, T.: A study on Caudrey–Dodd–Gibbon–Sawada–Kotera partial differential equation. *Math. Methods Appl. Sci.* **45**(14), 8737–8753 (2022a)
- Baskonus, H.M., Mahmud, A.A., Muhamad, K.A., Tanriverdi, T., Gao, W.: Studying on Kudryashov–Sinelnshchikov dynamical equation arising in mixtures liquid and gas bubbles. *Therm. Sci.* **26**(2B), 1229–1244 (2022b)
- Bilal, M., Haris, H., Waheed, A., Faheem, M.: The analysis of exact solitons solutions in monomode optical fibers to the generalized nonlinear Schrödinger system by the compatible techniques. *Int. J. Math. Comput. Eng.* **1**(2), 149–170 (2023). <https://doi.org/10.2478/ijmce-2023-0012>
- Chen, T.-T., Hu, P.-Y., He, J.-S.: General higher-order breather and hybrid solutions of the Fokas system. *Commun. Theor. Phys.* **71**(5), 496–508 (2019)
- Fokas, A.: On the simplest integrable equation in  $2+1$ . *Inverse Probl.* **10**(2), 19–22 (1994)
- Gasmi, B., Ciancio, A., Moussa, A., Alhakim, L., Mati, Y.: New analytical solutions and modulation instability analysis for the nonlinear  $(1+1)$ -dimensional phi-four model. *Int. J. Math. Comput. Eng.* **1**(1), 79–90 (2023). <https://doi.org/10.2478/ijmce-2023-0006>

- Ghanbari, B.: Abundant soliton solutions for the Hirota–Maccari equation via the generalized exponential rational function method. *Mod. Phys. Lett. B* **33**(09), 1950106–1950127 (2019)
- Ghanbari, B., Akgül, A.: Abundant new analytical and approximate solutions to the generalized Schamel equation. *Phys. Scr.* **95**(7), 075201–075221 (2020)
- Ghanbari, B., Baleanu, D.: New solutions of Gardner’s equation using two analytical methods. *Front. Phys.* **7**, 202–215 (2019)
- Ghanbari, B., Baleanu, D.: New optical solutions of the fractional Gerdjikov–Ivanov equation with conformable derivative. *Front. Phys.* **8**, 167–178 (2020)
- Ghanbari, B., Gómez-Aguilar, J.: Optical soliton solutions for the nonlinear Radhakrishnan–Kundu–Lakshmanan equation. *Mod. Phys. Lett. B* **33**(32), 1950402–1950417 (2019a)
- Ghanbari, B., Gómez-Aguilar, J.: New exact optical soliton solutions for nonlinear Schrödinger equation with second-order spatio-temporal dispersion involving m-derivative. *Mod. Phys. Lett. B* **33**(20), 1950235–1950254 (2019b)
- Ghanbari, B., Kuo, C.-K.: New exact wave solutions of the variable-coefficient  $(1+1)$ -dimensional Benjamin–Bona–Mahony and  $(2+1)$ -dimensional asymmetric Nizhnik–Novikov–Veselov equations via the generalized exponential rational function method. *Eur. Phys. J. Plus* **134**(7), 334–347 (2019)
- Ghanbari, B., Baleanu, D., Al Qurashi, M.: New exact solutions of the generalized Benjamin–Bona–Mahony equation. *Symmetry* **11**(1), 20–31 (2018)
- Iqbal, M., Seadawy, A.R.: Instability of modulation wave train and disturbance of time period in slightly stable media for unstable nonlinear Schrödinger dynamical equation. *Mod. Phys. Lett. B* **34**(supp01), 2150010–2150024(2020)
- Iqbal, M., Seadawy, A.R., Lu, D.: Construction of solitary wave solutions to the nonlinear modified Korteweg-de Vries dynamical equation in unmagnetized plasma via mathematical methods. *Mod. Phys. Lett. A* **33**(32), 1850183–1850195 (2018a)
- Iqbal, M., Seadawy, A.R., Lu, D.: Dispersive solitary wave solutions of nonlinear further modified Korteweg-de Vries dynamical equation in an unmagnetized dusty plasma. *Mod. Phys. Lett. A* **33**(37), 1850217–1850236 (2018b)
- Iqbal, M., Seadawy, A.R., Lu, D.: Applications of nonlinear longitudinal wave equation in a magneto-electro-elastic circular rod and new solitary wave solutions. *Mod. Phys. Lett. B* **33**(18), 1950210–1950226 (2019)
- Jafari, H., Goswami, P., Dubey, R.S., Sharma, S., Chaudhary, A.: Fractional SZIR model of zombie infection. *Int. J. Math. Comput. Eng.* **1**(1), 91–104 (2023). <https://doi.org/10.2478/ijmce-2023-0007>
- Khater, M.M.: Analytical simulations of the Fokas system; extension  $(2+1)$ -dimensional nonlinear Schrödinger equation. *Int. J. Mod. Phys. B* **35**(28), 2150286–2150301 (2021)
- Khater, M., Ghanbari, B.: On the solitary wave solutions and physical characterization of gas diffusion in a homogeneous medium via some efficient techniques. *Eur. Phys. J. Plus* **136**(4), 1–28 (2021)
- Kumar, S., Kumar, A.: Newly generated optical wave solutions and dynamical behaviors of the highly nonlinear coupled Davey–Stewartson Fokas system in monomode optical fibers. *Opt. Quantum Electron.* **55**(6), 566–598 (2023a)
- Kumar, A., Kumar, S.: Dynamic nature of analytical soliton solutions of the  $(1+1)$ -dimensional Mikhailov–Novikov–Wang equation using the unified approach. *Int. J. Math. Comput. Eng.* **1**(2), 217–228 (2023b). <https://doi.org/10.2478/ijmce-2023-0018>
- Lu, D., Seadawy, A.R., Iqbal, M.: Mathematical methods via construction of traveling and solitary wave solutions of three coupled system of nonlinear partial differential equations and their applications. *Results Phys.* **11**, 1161–1171 (2018)
- Mahmud, A.A.: Application of three different methods to several nonlinear partial differential equations modeling certain scientific phenomena. Ph.D. thesis (2023, Harran University, Faculty of Arts and Sciences, Department of Mathematics)
- Mahmud, A.A., Tanriverdi, T., Muhamad, K.A., Baskonus, H.M.: Characteristic of ion-acoustic waves described in the solutions of the  $(3+1)$ -dimensional generalized Korteweg-de Vries–Zakharov–Kuznetsov equation. *J. Appl. Math. Comput. Mech.* **22**(2), 36–48 (2023a)
- Mahmud, A.A., Tanriverdi, T., Muhamad, K.A.: Exact traveling wave solutions for  $(2+1)$ -dimensional Konopelchenko–Dubrovsky equation by using the hyperbolic trigonometric functions methods. *Int. J. Math. Comput. Eng.* **1**(1), 11–24 (2023b). <https://doi.org/10.2478/ijmce-2023-0002>
- Mahmud, A.A., Tanriverdi, T., Muhamad, K.A., Baskonus, H.M.: Structure of the analytic solutions for the complex non-linear  $(2+1)$ -dimensional conformable time-fractional Schrödinger equation. *Therm. Sci.* **27**(Spec. issue 1), 211–225 (2023c)
- Mahmud, A.A., Baskonus, H.M., Tanriverdi, T., Muhamad, K.A.: Optical solitary waves and soliton solutions of the  $(3+1)$ -dimensional generalized Kadomtsev–Petviashvili–Benjamin–Bona–Mahony equation. *Comput. Math. Math. Phys.* **63**(6), 1085–1102 (2023d)

- Mohammed, W.W., Al-Askar, F.M., Cesarano, C.: Solitary solutions for the stochastic Fokas system found in monomode optical fibers. *Symmetry* **15**(7), 1433–1447 (2023)
- Muhamad, K.A.: A study on some nonstandard partial differential equations. Ph.D. thesis, Harran University, Faculty of Arts and Sciences, Department of Mathematics (2023)
- Muhamad, K.A., Tanriverdi, T., Mahmud, A.A., Baskonus, H.M.: Interaction characteristics of the Riemann wave propagation in the  $(2+1)$ -dimensional generalized breaking soliton system. *Int. J. Comput. Math.* **100**(6), 1340–1355 (2023)
- Nasir, M., Jabeen, S., Afzal, F., Zafar, A.: Solving the generalized equal width wave equation via sextic-spline collocation technique. *Int. J. Math. Comput. Eng.* **1**(2), 229–242 (2023). <https://doi.org/10.2478/ijmce-2023-0019>
- Rao, J.-G., Wang, L.-H., Zhang, Y., He, J.-S.: Rational solutions for the Fokas system. *Commun. Theor. Phys.* **64**(6), 605–618 (2015)
- Rao, J., Mihalache, D., Cheng, Y., He, J.: Lump-soliton solutions to the Fokas system. *Phys. Lett. A* **383**(11), 1138–1142 (2019)
- Rao, J., He, J., Mihalache, D.: Doubly localized rogue waves on a background of dark solitons for the Fokas system. *Appl. Math. Lett.* **121**, 10743–107441 (2021)
- Rehman, S.U., Ahmad, J.: Diverse optical solitons to nonlinear perturbed Schrödinger equation with quadratic-cubic nonlinearity via two efficient approaches. *Phys. Scr.* **98**(3), 035216–035232 (2023)
- Rehman, S.U., Bilal, M., Ahmad, J.: The study of solitary wave solutions to the time conformable Schrödinger system by a powerful computational technique. *Opt. Quantum Electron.* **54**(4), 228–245 (2022)
- Rehman, S.U., Ahmad, J., Muhammad, T.: Dynamics of novel exact soliton solutions to stochastic chiral nonlinear Schrödinger equation. *Alex. Eng. J.* **79**, 568–580 (2023a)
- Rehman, S.U., Ahmad, J., Muhammad, T.: Dynamics of novel exact soliton solutions to stochastic chiral nonlinear Schrödinger equation. *Alex. Eng. J.* **79**, 568–580 (2023b)
- Seadawy, A.R., Iqbal, M.: Propagation of the nonlinear damped Korteweg-de Vries equation in an unmagnetized collisional dusty plasma via analytical mathematical methods. *Math. Methods Appl. Sci.* **44**(1), 737–748 (2021)
- Seadawy, A.R., Iqbal, M.: Dispersive propagation of optical solitons and solitary wave solutions of Kundu–Eckhaus dynamical equation via modified mathematical method. *Appl. Math.-A J. Chin. Univ.* **38**(1), 16–26 (2023)
- Seadawy, A.R., Iqbal, M., Lu, D.: Applications of propagation of long-wave with dissipation and dispersion in nonlinear media via solitary wave solutions of generalized Kadomtsev–Petviashvili modified equal width dynamical equation. *Comput. Math. Appl.* **78**(11), 3620–3632 (2019)
- Seadawy, A.R., Iqbal, M., Lu, D.: Construction of soliton solutions of the modify unstable nonlinear Schrödinger dynamical equation in fiber optics. *Indian J. Phys.* **94**, 823–832 (2020a)
- Seadawy, A.R., Iqbal, M., Lu, D.: Propagation of kink and anti-kink wave solitons for the nonlinear damped modified Korteweg-de Vries equation arising in ion-acoustic wave in an unmagnetized collisional dusty plasma. *Phys. A Stat. Mech. Appl.* **544**, 123560–123574 (2020b)
- Seadawy, A.R., Iqbal, M., Althobaiti, S., Sayed, S.: Wave propagation for the nonlinear modified Korteweg-de Vries Zakharov–Kuznetsov and extended Zakharov–Kuznetsov dynamical equations arising in nonlinear wave media. *Opt. Quantum Electron.* **53**, 1–20 (2021)
- Seadawy, A.R., Zahed, H., Iqbal, M.: Solitary wave solutions for the higher dimensional Jimo–Miwa dynamical equation via new mathematical techniques. *Mathematics* **10**(7), 1011–1025 (2022)
- Shafqat-ur-Rehman, Ahmad, J.: Stability analysis and novel optical pulses to Kundu–Mukherjee–Naskar model in birefringent fibers. *Int. J. Mod. Phys. B* 2450192–2450206 (2023)
- Srinivasa, K., Mundewadi, R.A.: Wavelets approach for the solution of nonlinear variable delay differential equations. *Int. J. Math. Comput. Eng.* **1**(2), 139–148 (2023). <https://doi.org/10.2478/ijmce-2023-0011>
- Tanriverdi, T., Baskonus, H.M., Mahmud, A.A., Muhamad, K.A.: Explicit solution of fractional order atmosphere-soil-land plant carbon cycle system. *Ecol. Complex.* **48**, 100966–100977 (2021)
- Tarla, S., Ali, K.K., Sun, T.-C., Yilmazer, R., Osman, M.: Nonlinear pulse propagation for novel optical solitons modeled by Fokas system in monomode optical fibers. *Results Phys.* **36**, 105381–105389 (2022)
- Thilakavathy, J., Amrutha, R., Subramanian, K., Sivatharani, B.: Plenteous stationary wave patterns for  $(2+1)$  dimensional Fokas system. *Phys. Scr.* **98**(11), 115226–115237 (2023)
- Wang, K.-J.: Abundant exact soliton solutions to the Fokas system. *Optik* **249**, 168265–168279 (2022)
- Wang, K.-J., Liu, J.-H., Wu, J.: Soliton solutions to the Fokas system arising in monomode optical fibers. *Optik* **251**, 168319–168330 (2022)
- Zhang, K., Han, T., Li, Z.: New single traveling wave solution of the Fokas system via complete discrimination system for polynomial method. *AIMS Math.* **8**(1), 1925–1936 (2023)

**Publisher's Note** Springer Nature remains neutral with regard to jurisdictional claims in published maps and institutional affiliations.

## Authors and Affiliations

**Adnan Ahmad Mahmud<sup>1</sup> · Kalsum Abdulrahman Muhamad<sup>1</sup> · Tanfer Tanriverdi<sup>1</sup> ·  
Haci Mehmet Baskonus<sup>2</sup>**

✉ Adnan Ahmad Mahmud  
mathematic79@yahoo.com

Kalsum Abdulrahman Muhamad  
kalsumabdulrahman58@gmail.com

Tanfer Tanriverdi  
ttanriverdi@harran.edu.tr

Haci Mehmet Baskonus  
hmbaskonus@gmail.com

<sup>1</sup> Department of Mathematics, Faculty of Arts and Sciences, Harran University, 63290 Şanlıurfa, Turkey

<sup>2</sup> Department of Mathematics and Science Education, Faculty of Education, Harran University, 63190 Şanlıurfa, Turkey